

Assessment of Dynamic Loads on Railway Bridges

H. Bigelow, B. Hoffmeister and M. Feldmann
Institute for Steel Structures
RWTH Aachen University, Germany

Abstract

The realistic assessment of dynamic loads on railway bridges can be very challenging. Depending on span and construction type there can be huge difference between predicted and measured response. Especially when comparing calculated and measured fundamental frequencies of short and medium single span filler beam bridges, measured values can sometimes be determined as twice as large as the calculated values.

A monitoring system installed on a filler beam bridge is used to investigate the dynamic behaviour of the bridge. Crossings of different train types with different velocities and the resulting accelerations und deformations are compared to the respective calculated ones. Several methods to include the influence of structural boundary conditions are checked against each other.

Furthermore fatigue phenomena are investigated, though for this particular filler beam bridge a fatigue check is not relevant for the dimensioning and in practice not required as there are no girder joints. The monitored load collectives are extrapolated to expected service life of one hundred years and compared to the load models for fatigue design. Additionally the performed fatigue check is used to assess if the fatigue check is justifiably not required.

Keywords: eigen frequency, damping, dynamic train load, resonance, bridges, filler beams, short and medium span, fatigue.

1 Introduction

Railway bridges are exposed to high dynamic loads resulting from regular train axle spacing combined with high velocities. With the increasing number of high-speed

rail links and technical developments allowing ever-higher velocities, raised requirements are placed on new-built and existing railway bridges.

Additionally the awareness of structural engineers of dynamic phenomena, especially resonance effects, has increased. While German railway bridges have been designed until 2000 considering equivalent static loads with dynamic magnification factors only, this approach has been restricted to certain conditions in present-day design process. In any other case additional explicit dynamic calculations with numerical models have to be performed.

2 Analysis

2.1 Railway loads on bridges

2.1.1 Dynamic effects

Dynamic design in general requires a careful consideration of possible resonance effects. Figure 1 depicts the dynamic magnification factor V for a single-degree-of-freedom-system. Though systems with more degrees of freedom and non-linear damping behaviour are discussed later on, this representation is very well suited for illustrating the resonance effect itself.

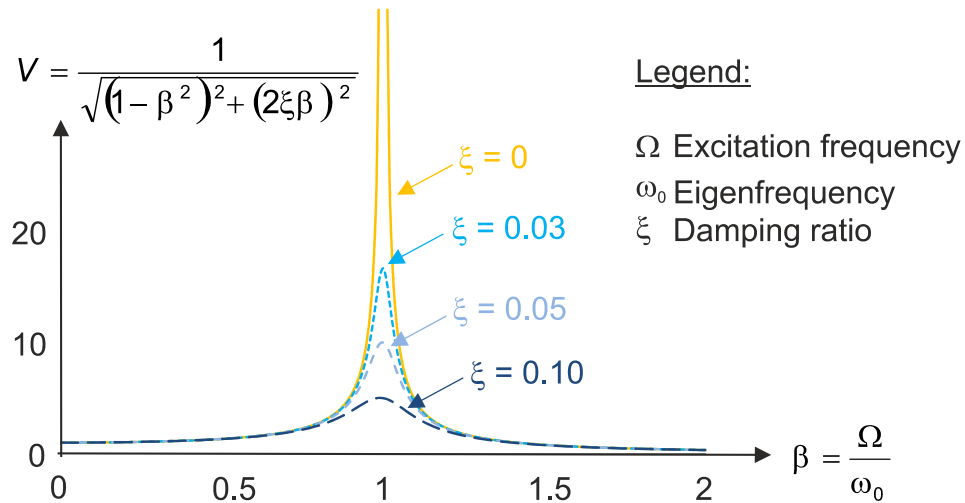


Figure 1: Magnification factor V

The dynamic magnification V is the ratio of a system's maximum reaction (usually deflection u), due to dynamic loading to the reaction due to the respective static one (for a more detailed explanation of the topic, see e.g. [15]):

$$V = \frac{u_{\max, \text{dynamic}}}{u_{\text{static}}} \quad (1)$$

Figure 1 outlines two important aspects of the resonance excitation: First, if Eigen frequency and excitation frequency are equal or very similar, the effects of dynamic load can be excessively higher than the corresponding static one.

Second, while the structure's damping capacity strongly influences the reaction to resonance excitation, there is hardly a difference between an undamped and a system with low (10 %) damping when subjected to excitation frequency, sufficiently different from the Eigen frequency.

When estimating the resonance risk, action side and resistance side of a structure have to be treated separately.

First it has to be checked if recurrent loads can cause an excitation frequency, which is the case for train loads due to their regular axle spacing. Then it has to be checked if this excitation frequency is likely to cause any resonance effects. For railway bridges this means taking into account (maximum) velocity and axle spacing of the crossing train as well as the structure's Eigen frequencies.

On the other side there are the structure's reaction and resistance, respectively. The structure's ability to withstand the resonance loading can be separated into its damping capacity and its structural components' resistances.

Railway bridges differ from other dynamically loaded structures such as foundations of industrial machinery with constant operating revolutions. They can be subjected to a number of different excitation frequencies due to different axle spacing of different train types and varying velocities. The relation between excitation frequency, axle spacing and train velocity is illustrated in the next section.

The structural damping of railway bridges is low. Current standards allow a consideration of not more than 3 % depending on bridge type, span, etc., see [7], [3]. Though measurements on existing bridges reveal that the codes' damping ratios are very conservative, the actual damping still has to be considered small. In scope of a metrological investigation of approx. 30 filler beam bridges for all of them damping ratios of less than 7 % were measured, see [19].

The duration of the excitation is limited though. This means, even if there is resonance excitation; it is followed by a free decay process after the train has left the bridge. This is a huge difference to the magnification factor V depicted in figure 1 displaying an excitation frequency Ω of infinite duration.

2.2.2 Simulation of train crossings

Train crossings cause excitation frequencies n_E depending on train velocity v and length over buffers $L_{üP}$, [1]:

$$n_E = \frac{v}{L_{üP}} \quad (2)$$

As figure 2 shows, the length over buffers, i.e. the length of the carriage, can be different for each train type.

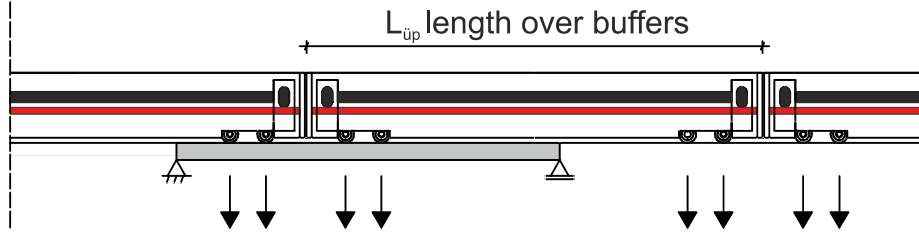


Figure 2: Length over buffers

For each train type expected to cross the respective bridge a series of simulations with varying velocities has to be performed. If interoperability criteria for the European high-speed traffic have to be fulfilled, additional load models HSLM (high speed load model) have to be considered, again with several simulations, [7]. Simulations can be performed with moving single loads or more complicated dynamic models, considering mass, inertia, spring and damper properties of the bogies and hence interaction between bridge and train, [1]. In case of a simulation with single loads, additional damping can be considered. The values are given in [7].

Corresponding to (2) for each train type critical velocities can be derived [3], where resonance effects have to be expected if the respective excitation frequency of the train equals one of the system's Eigen frequencies.

$$v_{res,i,k} = n_j \cdot \frac{L_{üP,k}}{i} \quad (3)$$

Where $v_{res,i,k}$ [m/s²] describes the i^{th} critical velocity of train type k with length over buffers $L_{üP,k}$ [m], depending on the j^{th} Eigen frequency n_j [Hz] of the bridge. The value i considers the fact, that resonance can also be excited by an integral multiple of the Eigen frequency; i is limited to 4.

Standards [7] and [3] define slightly different speed ranges to be investigated. While according to [7] velocities between 40 km/h and 1.2 times the local speed have to be considered, [3] defines the lower limit as the smaller value of $0.9 \cdot n_0 \cdot L_{üP,k}$ and [160 km/h (for passenger trains) or 90 km/h (for freight trains)], where n_0 is the fundamental Eigen frequency of the bridge.

Within the investigated speed range several simulations have to be performed. Again [7] and [3] differ from each other. In [7] a closer observation of velocities near the critical velocities is required, though there is no indication how many simulations in the complete speed range have to be performed. Only critical velocities depending on n_0 have to be considered.

[3] requires simulations in steps of 10 km/h within the total speed range and steps of 5 km/h near the critical velocities, which have to be considered for all Eigen frequencies $n_j \leq n_{max} = \max \{30 \text{ Hz}; 1.5 \cdot n_0; n_2\}$.

As the numeric simulation of so many train crossings is very costly and time consuming, the use of simplified verifications and equivalent static load models is very popular. As it is shown in the next section, their exclusive use is limited to certain fields of application only. Bridges dimensioned with dynamic calculations have additionally to be verified against the simplified load models as well.

The use of response spectra, e.g. [24], or tables summarizing maximum values [3] can reduce the workload. Results may be very conservative though. The problematic nature of a realistic assessment of the real bridge behaviour still remains.

For velocities greater than 160 km/h, the vertical accelerations have to be limited to 3.5 m/s² for bridges with ballast layers and 5 m/s² for bridges with slab tracks. If simplified verifications are applicable, this particular verification does not need to be performed.

2.2.3 Simplified verifications

Until 2000 German railway bridges have been dimensioned with the equivalent static load models LM 71, SW/0 and SW/2 combined with dynamic coefficients ϕ_2 (tracks with diligent maintenance) and ϕ_3 (tracks with regular maintenance) and load class coefficient α . In today's practice their exclusive use is limited to certain requirements defined in [7].

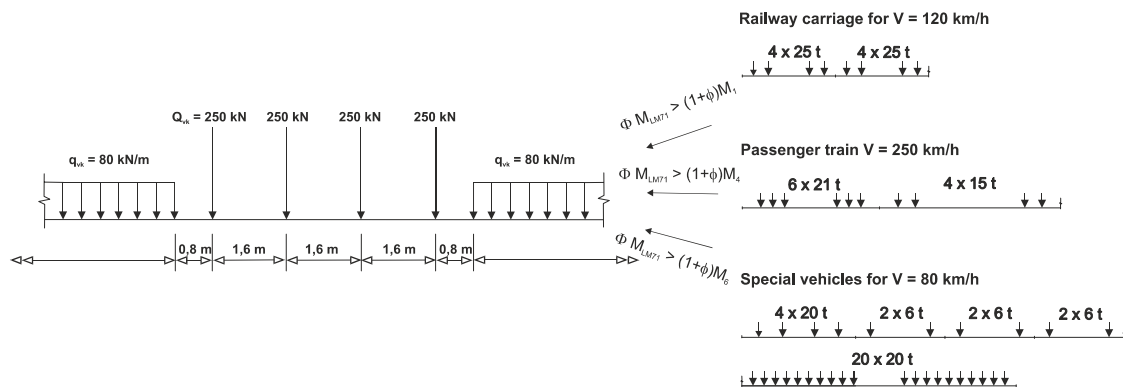


Figure 3: Static load model LM 71 and the three of six load models it is based on

Figure 3 depicts the static load model LM 71. In [16] the development of the LM 71 for passenger trains is described in detail. It is a fictitious load model based on six individual operating load trains, see e.g. [26]; each combined with dynamic load coefficients $(1 + \phi)$, considering a representative velocity for the respective train. The three decisive trains, LM71 was based on are also depicted in Figure 3.

The dynamic load coefficient $(1 + \phi)$ is still valid for the representation of the dynamic effects of individual trains with velocities up to 200 km/h and can be found in annex C of [7]. The coefficient takes the length over buffers and the velocity of the train as well as the fundamental Eigen frequency of the bridge into account.

Today's limits for the applicability of LM 71 and $(1 + \phi)$ can be explained by the assumptions, measurements and calculations their development was based on. For $(1 + \phi)$ measurements on 38 bridges with train velocities up to 240 km/h were taken as basis, [26]. A local velocity of 200 km/h times 1.2 equals the design velocity of 240 km/h.

Resonance effects were not taken into account, which explains why the resonance risk has to be ruled out. For single span bridges with velocities up to 200 km/h or

spans larger than 40 m, the resonance risk can be ruled out if the fundamental frequency n_0 is between two boundary values, as depicted in figure 4.

In [7] a flow chart is depicted to decide if a dynamic calculation is required or if the use of simplified verifications is possible.

2.2 Fatigue of railway bridges

2.2.1 General

Verifications against fatigue of railway bridges are specified in [7] with references to [8], [9] and [11]. Again it has to be differentiated between the assessment with simplified load models and additional dynamic calculations. Railway bridges are designed for a service time of 100 years.

2.2.2 Simulation of train crossings for fatigue

If the traffic loads resulting from train crossings on a bridge have to be calculated by explicit dynamic calculations as shown in the sections above, [7] requires verifications additional to those described in the following section.

All oscillation amplitudes have to be taken into account, including those of the bridge's free decay process. The expected traffic composition and yearly tonnage can be defined as well as frequent train velocities. Otherwise a number of train crossings with velocities up to the local velocity have to be checked. If the local velocity is near one critical velocity for a certain train type, the resonance effects have to be considered in the verification against fatigue.

2.2.3 Simplified load models for fatigue

[7] defines standard traffic on railway bridges as the traffic based on characteristic values of the load models LM 71 and SW, combined with ϕ . As verification against fatigue with the actual standard load models leads to unnecessarily unfavourable results, annex D specifies alternative train types for the assessment of fatigue.

The bridge has to be categorised into D.1 (regular traffic), D.2 (heavy traffic with 250 kN axles) or D.3 (local traffic). For each category train types, velocities, number of trains per day and yearly tonnage is defined. The yearly tonnage per rail is about 25×10^6 t. The static train loads have to be multiplied with dynamic coefficients $1 + \frac{1}{2} (\varphi' + \frac{1}{2} \varphi'')$. These dynamic coefficients for individual trains are different from those to be used for verifications in the ultimate limit state. Alternative traffic compositions can be defined by the client.

As can be seen in the next sections, the respective standards always refer to the simpler but unfavourable verification with ϕ times LM71, before referring to the fatigue load models from annex C. There are 12 train types of which depending on bridge category at least four have to be considered. The regular traffic even requires the consideration of eight load models.

2.2.4 Steel bridges

According to [7], steel bridges are verified against fatigue by means of:

$$\gamma_{Ff} \cdot \lambda \cdot \phi_2 \cdot \Delta\sigma_{71} \leq \frac{\Delta\sigma_c}{\gamma_{Mf}} \quad (4)$$

Where the recommended value for γ_{Ff} is 1.0, λ is the coefficient for damage equivalent specified in [10], ϕ_2 is the dynamic coefficient and $\Delta\sigma_{71}$ is the stress range due to LM 71 or SW/0 (if required). The reference value for fatigue strength $\Delta\sigma_c$ and the respective safety factor γ_{Mf} are defined in [9].

Formula (4) corresponds to the simplified fatigue verification according to [10]. Alternatively [10] allows the calculation of stress range spectra by interpretation of stress time histories. According to [9], annex A stress range spectra can be determined by rainflow or reservoir analyses of all relevant notch details.

Cumulative damage is verified against with:

$$D_d = \sum_i^n \frac{n_{Ei}}{N_{Ri}} \leq 1 \quad (5)$$

Where n_{Ei} is the number of stress ranges $\gamma_{Ff} \cdot \Delta\sigma_i$ and N_{Ri} is the durability obtained from the respective Woehler line.

2.2.5 Concrete bridges

Concrete bridges have to be verified against fatigue according to the specifications defined in [8]. Again it can be chosen between the simplified (unfavourable) approach with $\phi \cdot LM71$ and the more complicated approach considering cumulative damage with the Palmgreen-Miner method. The formula is analogue to formula (5). The resistance against fatigue of the compressed concrete is determined by:

$$N_i = 10^{\left(14 \frac{1 - E_{cd,max,i}}{\sqrt{1 - R_i}}\right)} \quad (6)$$

Thus taking into account maximum concrete compressive stress level $E_{cd,max,i}$ and the ratio R_i of minimum to maximum compressive strength.

2.2.6 Composite bridges

In [11] additional specifications for verifications against the fatigue of headed studs are defined. For further verifications of concrete or steel, references to [8], [9] and [10] are made.

Composite filler beams are a special construction type consisting of several steel girders embedded in concrete. For this type of bridge no verification of the fatigue strength is required as long as there are no welded joints in the steel girders, [3].

2.3 Filler beam bridges

2.3.1 Assessment of filler beam bridges

Composite filler beam bridges are very common in the German railway network. First introduced to the railway network at the end of the 19th century, this construction type is still very popular for new and replacement bridges today, thus providing about a quarter of all German railway bridges. In [19] their history is summarised and a more detailed description of the construction type is given.

Figure 6 shows a typical twin composite filler beam bridge consisting of two separate decks divided by a gap. The ballast layer is continuous though. Alternatively filler beam bridges can be engineered with both tracks on one continuous superstructure.

Despite the popularity of filler beam bridges, a correct prediction of their dynamic properties and reactions to crossing trains is nevertheless challenging. Especially bridges with short and medium spans have proven to be very resonance-prone when assessed by calculations only.

As it was mentioned in section 2.2.3, the resonance risk of single span bridges with velocities up to 200 km/h or minimum spans of 40 m can be ruled out if the fundamental Eigen frequencies are between the two boundary limits depicted in figure 4. Calculated and measured fundamental Eigen frequencies of 30 filler beam bridges [19] have been added to the diagram.

While the calculated values are smaller than the lower limit, the corresponding measured ones lie between both limit values. The investigated bridges were dimensioned before the year 2000 with equivalent static load models only. When the train type ICE 3 was introduced resonance was expected and the metrological investigations were carried out. Afterwards the bridges were opened to traffic with velocities over 200 km/h.

Many researchers have already identified not taking the influence of structural boundary conditions into account as one of the many reasons for differences between calculated and measured values.

To study the influence of the structural boundary conditions on the bridge behaviour a permanent monitoring system on a filler beam bridge was installed.

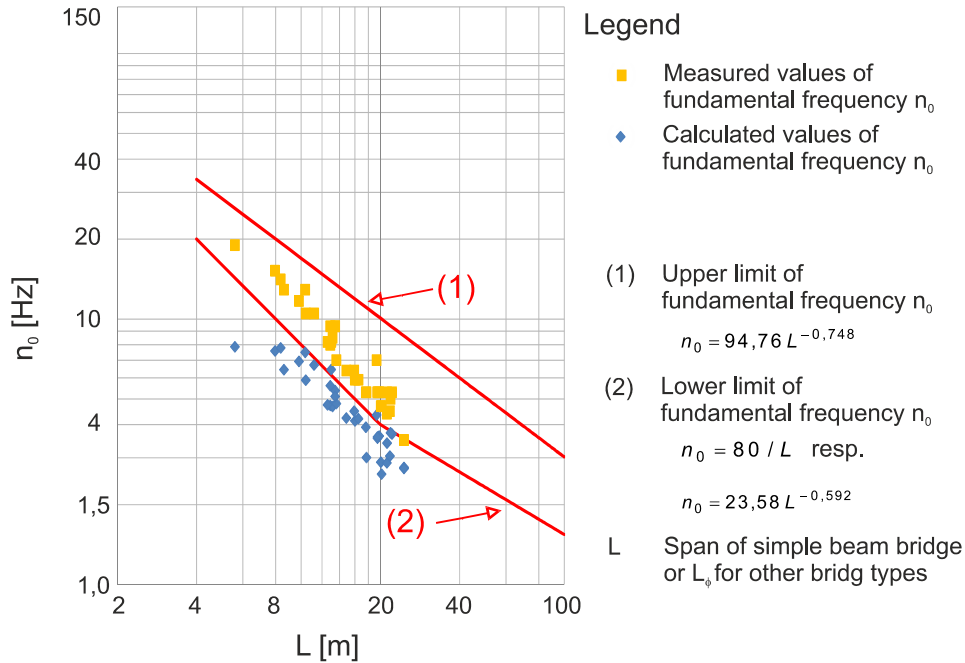


Figure 4: Limits for fundamental Eigen frequency n_0 according to [7] as well as measured and calculated values of filler beam bridges

3 Monitoring on a filler beam bridge

3.1 Description of the bridge and technical equipment

A permanent monitoring system was installed on German railway bridge EÜ Erfttalstraße. The bridge is part of the European high speed railway network connecting Paris, Brussels and Cologne. The bridge is located in Kerpen, near Cologne. This particular track section is used by high-speed passenger trains ICE and Thalys with maximum velocities of 250 km/h as well as slower traveling local passenger and freight trains.

The bridge EÜ Erfttalstraße was chosen from the 30 filler beam bridges mentioned in the sections above.

The bridge is a typical twin composite filler beam bridge with continuous ballast, see figure 5. With a span of 24.6 m it can be categorized as a medium span filler beam bridge showing considerable influences of structural boundary conditions as demonstrated in the subsequent sections.

The two superstructures are offset by four meters in longitudinal direction.

44 measuring points were installed on the bridge thus monitoring tri-axial accelerations in all 44 points and strains in all points except those located in the bearing axes; see Figure 6

The installation of the system was part of the RFCS (Research Found for Coal and Steel) project DETAILS [5]. More detailed descriptions of the instrumentation of the monitoring system are given in [17], [21], [22], [23].

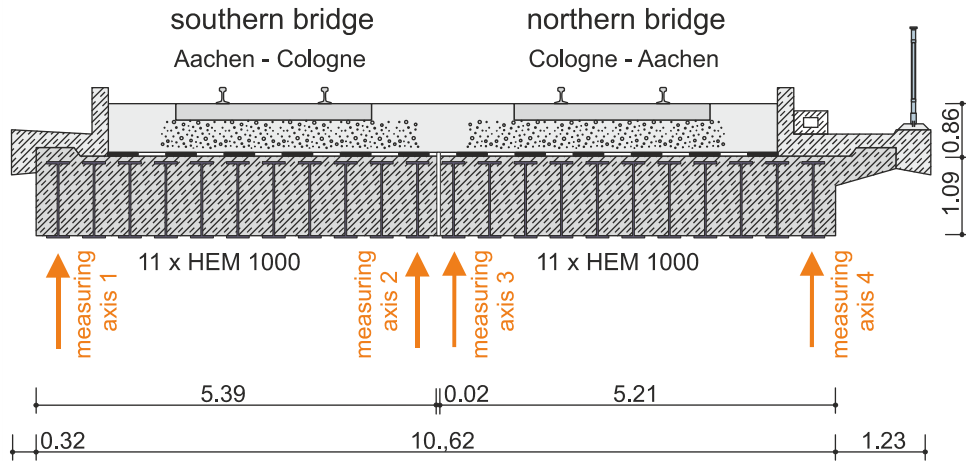


Figure 5: Cross section of the bridge Erfttalstraße with measuring axes

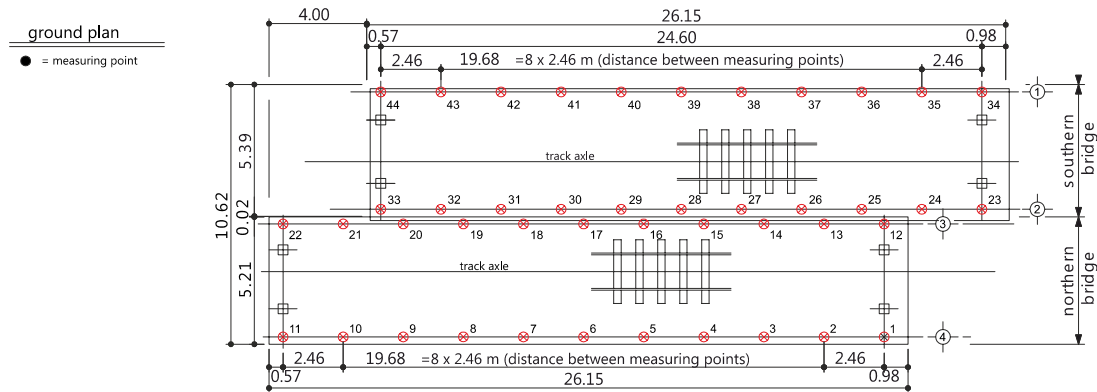


Figure 6: Measuring points bridge Erfttalstraße

3.2 Evaluation of measurement results

Measurement data were recorded between 2009 and 2011, though data logging could not be provided for the entire period. Nevertheless a sufficient number of train passages could be recorded to study typical characteristics of structural boundary conditions including seasonal or weather dependant effects.

The results have been partially published, most recently in [2]. This publication focuses on the fatigue aspect, though short summary of the known phenomena is given and reference to more detailed descriptions is made.

Deflection time histories can be calculated from the measured strain time histories using a conversion algorithm. The algorithm in style of the finite element method transfers a vector containing strains of one measuring axis (e.g. points 2 to 10 in axis 4) into a vector with the vertical deflections at these points. The method considers a condensed stiffness matrix and the distance h_0 between the strain gauge (at the steel

girder bottom edge) and the neutral axis. The derivation of the algorithm can be found in [22]. The method was verified on a downscaled model of the bridge in [21], while the values h_0 used for the individual axes are given in [17]. It has to be noted that h_0 slightly varies between the four axes as it depends on the geometry of the effective cross section influenced by the additional structural elements.

As mentioned in [17], an evaluation routine [12] programmed in MATLAB [14] was used to identify for each train crossing: train type and velocity, maximum strain, acceleration and deflection as well as damping ratio and fundamental Eigen frequency.

The upgrading process of the evaluation routine is still going on, [27]. The most recent development is an implementation of a Rainflow-HCM algorithm as described in [3] for the evaluation of load collectives.

3.3 Comparison of measurements and standards

3.3.1 Effects of structural boundary conditions

According to current standards only the contribution of the filler beam bridge superstructure to the moment of inertia I may be considered.

This applies both to formula (7) [4] for calculating the fundamental Eigen frequency n_0 of a single span bridge of length L and to the numeric modelling of bridges.

$$n_0 = \frac{\pi}{2L^2} \sqrt{\frac{EI}{m}} \quad (7)$$

The contribution of structural elements such as concrete edge-caps, rails or ballast layer to the mass m has to be considered though. Most of the structural boundary elements of a typical filler beam bridge are depicted in Figure 5; elastomeric bearings are not pictured though.

In [4] recommendations for the numerical modelling of railway bridges are given, indicating the possibility of a more realistic representation of the fundamental Eigen frequency, especially for filler beam bridges. Consideration of rails and real bearing conditions, different from the ideal hinge, is suggested.

To consider the influence of the rails, a separate modelling of rails and superstructure is advised; where the rails are modelled as beam elements, connected to the superstructure via spring elements representing the ballast. The non-linear spring law, to be obtained from [7], represents the displacement resistance of the rail-ballast-bridge system in longitudinal direction.

Bearing conditions differ from the ideal hinged representation due to restoring moments and forces in the elastomeric bearing combined with offset between neutral axis and bearing axis.

As shown in [20] the separate modelling of rails and superstructure increases only slightly the computed value of n_0 . Calculated maximum bending moments due to

train crossings can be more clearly decreased. Nonetheless the achievable reductions there do not justify the drastically raised computational time. In addition to the bridge Efrttalstraße five other filler beam bridges were numerically investigated.

The consideration of restoring forces in the bearings does have hardly any effect. For 11 filler beam bridges it could be shown in [20], that the influence on n_0 and maximum bending moments is negligible.

The contribution of the Concrete edge-caps and protective layer to the stiffness has been investigated by several researchers, though mostly on single bridges.

In [20] two approaches to include the additional stiffness have been applied and compared to values calculated according to standards as well as measured values of n_0 of 9 bridges. In Figure 7 the respective values for the bridge Efrttalstraße are presented.

First the additional stiffness of the caps and layers were analysed, assuming flexible shear bonding between these elements and the superstructure. This already displayed a slight improvement of the calculated fundamental frequencies.

Afterwards a rigid shear connection was assumed by which very good results could be achieved. The thus calculated fundamental Eigen frequencies are still smaller than the measured ones but sufficiently similar to the measured values. The computational resonance risk according to the formulas depicted in Figure 4 can be ruled out with consideration of the additional stiffness. In [25] this approach was investigated for bridges with fixed tracks without ballast layer.

Comparing recorded deflection and acceleration time-histories of the bridge Efrttalstraße to numeric simulations with the two approaches and values calculated according to standards showed a very good approximation of the numeric simulations assuming a rigid connection, especially during the train passage. In [20] the results for train passages of German high-speed train ICE 3 with $v = 245$ km/h and local passenger train RE with $v = 130$ km/h are presented. In figure 8 the ICE 3 train passages are presented once more.

Furthermore in Figure 7 it is shown for a wider range of velocities that assuming a rigid connection leads to a good approximation of calculated to measured results, still larger than the calculated ones and thus suited for a safe dimensioning of railway bridges.

The influence of the ballast layer on the structural behaviour of the bridge is described detailed in [18]. There the interaction effect between two superstructures divided by a gap but with continuous ballast was experimentally investigated. Stiffness parameters of the ballast with and without this coupling effect could be obtained experimentally.

During the train passage on the loaded deck, a reaction of the unloaded deck can be noticed. After the train has left the bridge, both decks oscillate in a mutual free decay process.

Applying the coupling effect combined with additional stiffness of the caps and protective layer to numerical models, led to unsafe results during the train passage, but to very good results modelling the decay process, [20]. This emphasises the non-

linear stiffness contribution of the ballast layer described in [18]: Higher oscillation amplitudes lead to destabilisation of the ballast resulting in lower stiffness but higher damping; while smaller amplitudes show higher stiffness but lower damping.

A consideration of additional stiffness of the boundary elements and the coupling effect during the train passage as described before is therefore not advisable for the dimensioning of the bridge as can be seen in Figure 7. It only applies to the free decay process which is unimportant for the determination of relevant internal forces.

In [20] and [17], respectively a method is introduced to consider the influence of the structural boundary elements by applying a correction factor k_E to the conventionally calculated bending stiffness EI_{cal} to assess the effective stiffness EI_{eff} of filler beam bridges as can be seen in formula (8):

$$EI_{eff} = EI_{cal} \cdot k_E \cdot \kappa_E \quad (8)$$

The security factor κ_E is 0.9 for new bridges and 1.0 for already existing ones. The correction factor k_E varies between 1.5 and 3.0 depending on the bridge span, thus considering the higher influence of the structural boundary elements on short bridges with spans $L < 10 \text{ m}$.

This method is valid for the calculation of n_0 according to formula (7) and the simulation of train passages with numerical models. The results obtained were checked against measured values.

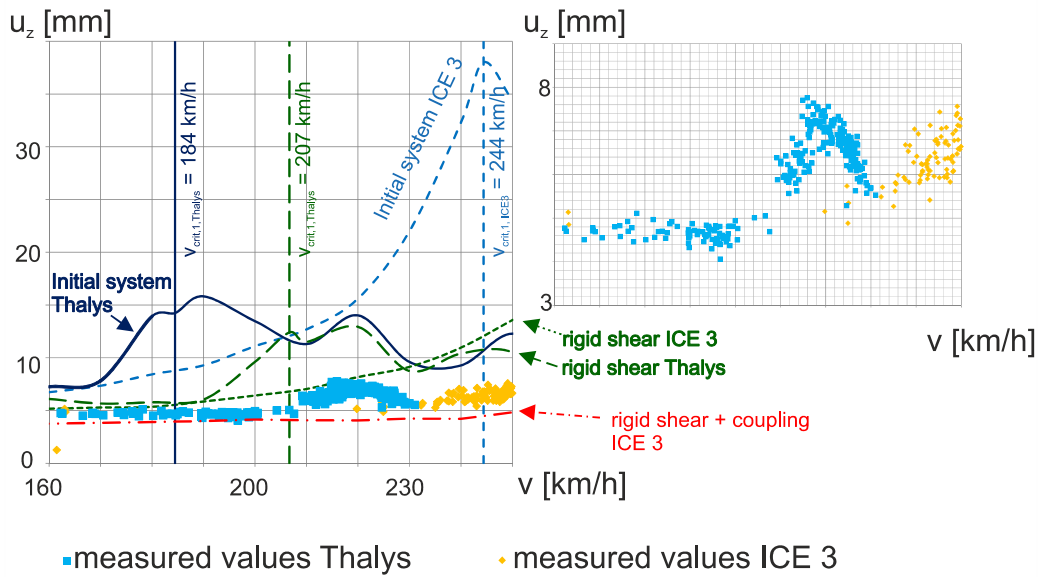
In Figure 7 monitored maximum deflections, resulting from passages of the high-speed trains ICE 3 and Thalys are plotted over the respective train velocities. Only results of the northern bridge deck are presented. The respective results monitored on the southern bridge deck, as well as maximum accelerations, fundamental Eigen frequencies and damping ratios of these train passages are given in [2].

Additionally the maximum deflections obtained from calculations performed with the program InfoCAD [13] are presented. A detailed description of the implementation of the different numerical models is given in [20].

The deflections caused by train passages obtained from a model with just the stiffness properties of the superstructure according to standards are unrealistically larger than the measured ones. The consideration of the additional stiffness properties of the caps and the protective layer not only decreases the maximum deflection values but also shifts the critical velocities into the range of the measured ones. The values obtained this way are still larger than the measured ones making them valid for dimensioning, while consideration of additional stiffness and coupling effect from ballast leads to unsafe results.

The plots show various phenomena. The strong dependency of the deflections on the train velocity is clearly evident. Moreover the different critical velocities according to formula (3) for different train types with different carriage lengths can be seen.

Maximum measured and calculated deflections
Northern bridge - Erfthalstraße



	Initial system	additional stiffness - flexible shear	additional stiffness - rigid shear	measured value
Northern bridge	$n_0 = 2.74$ Hz	$n_0 = 2.84$ Hz	$n_0 = 3.07$ Hz	$n_0 = 3.50$ Hz
Southern bridge	$n_0 = 2.76$ Hz	$n_0 = 2.84$ Hz	$n_0 = 3.22$ Hz	$n_0 = 3.50$ Hz

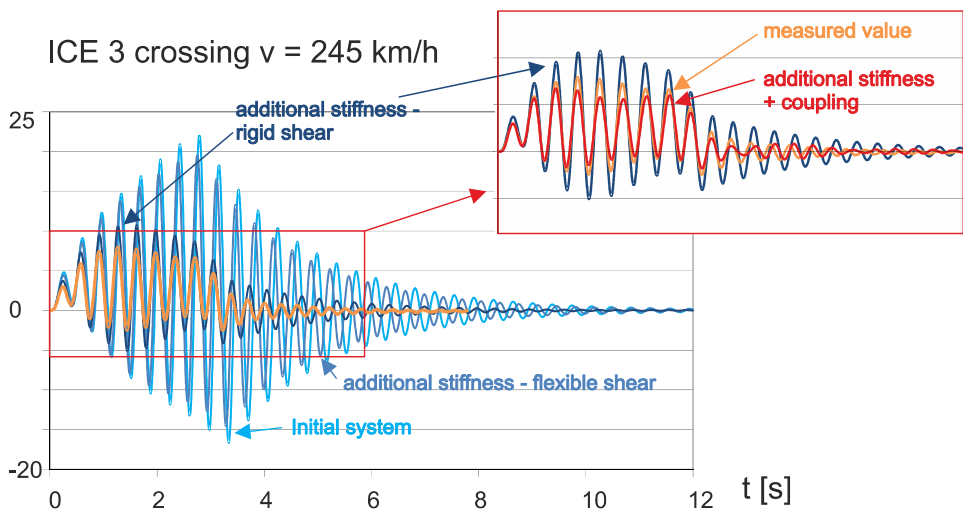


Figure 7: Measured and calculated data bridge Erfthalstraße

While maximum measured deflections of ICE 3 passages increase towards the speed limit of 250 km/h, a clear maximum near the critical Thalys velocity of $V_{res,1,Thalys} = 3.5 \cdot 18.7 = 65.45 \text{ m/s} = 236 \text{ km/h}$ can be seen, with respect to the measured fundamental frequency $n_0 = 3.5 \text{ Hz}$. The respective value for the ICE 3 is $V_{res,1,ICE\ 3} = 3.5 \cdot 24.775 = 86.7 \text{ m/s} = 312 \text{ km/h}$.

It is interesting though; that the maximum of the Thalys deflections does not exactly match the critical velocity, a phenomenon that can be noticed for the two calculated curves as well.

The calculated ICE 3 deflections on the other hand have their maximum at the respective critical velocity, making the difference between the train types evident.

As can be seen in Figure 7, the measured deflections scatter very much. Seasonal effects were observed as well. The fundamental frequencies in winter can be slightly higher due to freezing of the ballast layer, [2], [17]. Also slight differences could be noted depending on the time of the day.

3.3.2 Assessment of fatigue

As mentioned before, filler beam bridges without girder joints do not need to be verified against fatigue. Nonetheless a fatigue resistance check of the bridge Erfttalstraße with $\phi \cdot LM71$ is carried out.

The maximum bending moment M_{LM71} in mid-span of the 24.6 m long bridge Erfttalstraße resulting from load model LM 71 can be calculated as $M_{LM71} = 8662.4 \text{ kNm}$. For the verification against fatigue this value has to be multiplied with the dynamic coefficient $\phi_2 = 1.12$.

In Table 1 the respective input values for the resistance checks are presented, including selected intermediate values; separately for the southern and northern bridge decks. Apart from the slightly different dimensions (see Figure 5), the southern deck has concrete class B25, while the northern one has B35.

The composite neutral axis of the cross section is denoted as $h_{i,d}$, formulas for the determination of the geometric properties of filler beams are e.g. given in [4].

The verifications are all clearly fulfilled. The rolled steel girders fall into notch detail class 160, as there are no joints. In that case a lower notch detail class would have to be chosen and the verification provided against that value.

It is justified, that a fatigue check of filler beam bridges without welded joints is not required according to [4]. This complies with the reference in [11], annotating special cases where no further verification of fatigue strength is required except those specified in [9]. In other words no verification of the concrete is required, headed studs are non-existent and only the steel girders have to be checked.

As a next step the monitored load collectives of the bridge Erfttalstraße have been investigated. All 44 measuring points have been studied. Strain time-histories, measured during two representative days have been used to calculate the relevant steel tensile stresses and concrete compressive stresses. The results from these two days have been extrapolated to an expected service life of 100 years.

	Southern bridge	Northern bridge
Moment of inertia –composite cross section $I_i [m^4]$	0.993	0.908
Position of neutral axis $h_{i,d} = z_{Concrete} [m]$	0.546	0.545
$z_{Steel} [m]$	0.544	0.545
$\sigma_{Steel,LM71} [MN/m^2]$	48.554	53.260
$\sigma_{Concrete,LM71} [MN/m^2]$	-6.964	-8.611
Check of steel stresses according to formula (4)		
$\gamma_{Ff} \cdot \lambda \cdot \phi_2 \cdot \Delta\sigma_{LM71} [MN/m^2] \leq \Delta\sigma_C / \gamma_{Mf}$	$36.517 \leq 160/1.25 = 128$	$40.056 \leq 128$
Check of concrete Stresses according to [8]		
$14 \cdot \frac{1 - E_{ed,max,equ}}{\sqrt{1 - R_{equ}}} \geq 6$	$14.12 \geq 6$	$14.09 \geq 6$

Table 1: Input values simplified fatigue check bridge Erfttalstraße

All steel stresses are below the threshold value for the fatigue strength $\Delta\sigma_L$ according to [9] and therefore do not have to be considered.

The highest cumulative concrete damage was detected in measuring points 6 (south) and 39 (north), respectively, see Figure 6. The results are presented in Table 2, where it is distinguished between damage obtained from passages of 131 local trains RE, 13 high speed trains ICE, 17 high speed trains Thalys, 52 freight trains GUE, 9 individual engines and 27 not clearly identifiable trains, summarized as REST and 9 cases of simultaneous passages SIM on both decks.

The cumulative damage is very low, again proving that a fatigue check of filler beam bridges is justifiably not required.

4 Summary and outlook

The behaviour of filler beam bridges subjected to dynamic train loads has been described. Differences between calculated and measured fundamental frequencies, damping ratios, deflections and accelerations have been shown, giving special attention to resonance phenomena.

	Southern bridge (6)	Northern bridge (39)
RE: $\sum_{i=1}^{17} \frac{n_i}{N_i}$	3,71E-11	3,64E-11
ICE: $\sum_{i=1}^{13} \frac{n_i}{N_i}$	4,77E-12	4,92E-12
THALYS: $\sum_{i=1}^{17} \frac{n_i}{N_i}$	6,16E-12	5,35E-12
GUE: $\sum_{i=1}^{52} \frac{n_i}{N_i}$	1,75E-11	1,96E-11
REST: $\sum_{i=1}^{36} \frac{n_i}{N_i}$	9,41E-12	6,79E-12
SIM: $\sum_{i=1}^9 \frac{n_i}{N_i}$	4,28E-12	3,79E-12
\sum 2 days:	7,92E-11	7,68E-11
\sum 100 years:	1,45E-06	1,4011E-06

Table 2: Monitored cumulative concrete damage $\sum_{i=1}^m \frac{n_i}{N_i}$ Erfittalstraße

The differences are caused by the influence of structural boundary elements, which were further investigated by measurements obtained from a monitoring system installed on the German filler beam bridge Erfittalstraße

The characteristics of the individual boundary elements have been described and possibilities to include their influence into dynamic calculations have been discussed.

The influence of the boundary elements is currently being investigated more detailed in scope of the German research project DYNABRIDGE [6], funded by the Research Association Steel Application FOSTA. The project aims at the separation of permanent and only temporarily occurring effects. This will allow for the consideration of the permanent effects within the dimensioning process.

This means e.g. seasonal effects on the stiffness as ballast layer freezing have to be ruled out as well as effects changing the stiffness during the day. The latter could be caused by a prestressing effect in the concrete due to the more rapid cooling of steel. Nevertheless measured vehicle loads on the bridge will be included into this consideration as the monitoring already revealed larger deflections due to passages of local trains during commuting times.

In addition to this the fatigue behaviour of filler beam bridges has been investigated. As expected the bridges show an excellent resistance, not only in theory, when subjected to unfavourable fatigue load models but also assessed by real monitoring results.

References

- [1] L. Bagayoko, E. Koch, R. Patz: „Dynamik von Eisenbahnbrücken“, Stahlbau-Kalender 2008, ISBN: 978-3-433-01872-9, Ernst und Sohn, Berlin.
- [2] H. Bigelow, B. Hoffmeister, M. Feldmann, „Dynamic design of single span railway bridges with short and medium spans for high-speed“, VDI-Berichte Nr. 2160, S. 497-506, Kassel, 2012
- [3] U. H. Clormann, T. Seeger: „Rainflow-HCM, Ein Zählverfahren für Betriebsfestigkeitsnachweise auf werkstoffmechanischer Grundlage“, Stahlbau 3/1986, 65-71.
- [4] DB Netz AG: Richtlinie 804 Eisenbahnbrücken (und sonstige Ingenieurbauwerke) planen, bauen und instand halten, 2003.
- [5] DETAILS: Design for optimal life cycle costs (LCC) of high-speed railway bridges by enhanced monitoring systems, RFCS-project RFSR-CT-2006-2009.
- [6] DYNABRIDGE Dynamische Auslegung von Eisenbahn-Verbundbrücken mit kleinen und mittleren Spannweiten für den Hochgeschwindigkeitsverkehr, FOSTA P941, 2012-2013
- [7] Eurocode 1: Actions on structures - Part 2: Traffic loads on bridges, German version EN 1991-2:2003 + AC: 2010.
- [8] Eurocode 2: Design of concrete structures – Part 2: Concrete bridges – Design and detailing rules; German version EN 1992-2:2005 + AC:2008.
- [9] Eurocode 3: Design of steel structures - Part 1-9: Fatigue; German version EN 1993-1-9:2005 + AC:2009.
- [10] Eurocode 3: Design of steel structures - Part 2: Steel Bridges; German version EN 1993-2:2006 + AC:2009.
- [11] Eurocode 4: Design of composite steel and concrete structures – Part 2: General rules and rules for bridges; German version EN 1994-2:2005 + AC:2008.
- [12] FOX – evaluation routine monitoring Erfttalstraße, program version 1.40, F. Weil, T. Rauert, Institute for Steel Structures of the RWTH Aachen University, 2010.
- [13] InfoCAD program version 8.11e, Infograph GmbH, www.infocad.de, 2009.
- [14] MATLAB program version R2010b, MathWorks, 2010.
- [15] K. Meskouris: „Structural Dynamics: Models, Methods, Examples“, ISBN 3-433-01327-6, Ernst und Sohn, 2000.
- [16] G. Prommersberger, H. Siebke: “Das Belastungsbild UIC 71, die neue Bemessungsgrundlage für den Eisenbahnbrückenbau“, Eisenbahntechnische Rundschau (25), 1/2-1976.
- [17] T. Rauert: „Zum Einfluss baulicher Randbedingungen auf das dynamische Verhalten von WIB-Eisenbahnbrücken“, Schriftenreihe des Lehrstuhls für

- Stahlbau und Leichtmetallbau der RWTH Aachen, Heft 72 - 2011, D82 (Diss RWTH Aachen University, 2011), Shaker Verlag; ISBN 978-3-8440-0360-4..
- [18] T. Rauert, H. Bigelow, B. Hoffmeister, M. Feldmann: „On the prediction of the interaction effect caused by continuous ballast on filler beam railway bridges by experimentally supported studies“, *Engineering Structures* 32 (2010), 3981-3988.
- [19] T. Rauert, H. Bigelow, B. Hoffmeister, M. Feldmann, R. Patz, P. Lippert, „Zum Einfluss baulicher Randbedingungen auf das dynamische Verhalten von WiB-Eisenbahnbrücken, Teil 1: Einführung und Messuntersuchungen an WiB-Brücken“, *Bautechnik* 87 (2010), Heft 11, S. 665-672.
- [20] T. Rauert, H. Bigelow, B. Hoffmeister, M. Feldmann, R. Patz, P. Lippert, „Zum Einfluss baulicher Randbedingungen auf das dynamische Verhalten von WiB-Eisenbahnbrücken, Teil 2: Numerische Untersuchungen und Bemessungsvorschläge“, *Bautechnik* 87 (2010), Heft 12, S. 751-760.
- [21] T. Rauert, M. Feldmann, L. He, G. De Roeck, „Calculation of bridge deformations due to train passages by the use of strain and acceleration measurements from bridge monitoring supported by experimental tests“, *Proceedings of the 8th International Conference on Structural Dynamics, EURODYN 2011*, Leuven, Belgium.
- [22] T. Rauert, B. Hoffmeister, „Long-term monitoring of a twin composite filler beam railway bridge with continuous ballast“, *ISEV2009- Environmental Vibration: Prediction, Monitoring and Evaluation*.
- [23] T. Rauert, B. Hoffmeister, R. Cantieni, M. Brehm, V. Zabel, „Experimental Modal Analysis of a Twin Composite Filler Beam Railway Bridge for High-Speed Trains with Continuous Ballast“, *IABMAS Conference 2008*, Seoul, Korea.
- [24] M. Spengler: „Dynamik von Eisenbahnbrücken unter Hochgeschwindigkeitsverkehr - Entwicklung eines Antwortspektrums zur Erfassung der dynamischen Tragwerksreaktion“, *Institut für Massivbau, Technische Universität Darmstadt*; Heft 19; D17 (Diss TU Darmstadt, 2010), ISBN 978-3-9811881-6-5.
- [25] M. Spengler, H. Duda, C. A. Graubner, „Beanspruchung von Eisenbahnbrücken durch Hochgeschwindigkeitszugverkehr, Einfluss der Oberbauart „Feste Fahrbahn“ auf die strukturdynamischen Eigenschaften und die dynamische Tragwerksreaktion“, *VDI Berichte Nr. 1941*, 2006.
- [26] UIC-Codex 776-1, UIC – Union Internationale des Chemins de fer, International Union of Railways, 5th edition, 2007.
- [27] F. Weil: „Auswertung von Monitoring-Ergebnissen einer WiB-Eisenbahnverbundbrücke“, *Bachelor Thesis, Institute for Steel Structures, RWTH Aachen University*, 2012.